Mon. Not. R. Astron. Soc. **384,** 150–160 (2008) doi:10.1111/j.1365-2966.2007.12675.x

The LuckyCam survey for very low mass binaries – II. 13 new M4.5–M6.0 binaries⋆

N. M. Law,[1,2]† S. T. Hodgkin[2] and C. D. Mackay[2]

[1]*Department of Astronomy, Mail Code 105-24, California Institute of Technology, 1200 East California Blvd., Pasadena, CA 91125, USA*
[2]*Institute of Astronomy, University of Cambridge, Madingley Road, Cambridge CB3 0HA*

Accepted 2007 October 30. Received 2007 October 11; in original form 2007 April 17

ABSTRACT

We present results from a high angular resolution survey of 77 very low mass (VLM) binary systems with $6.0 \leqslant V-K$ colour $\leqslant 7.5$ and proper motion $\geqslant 0.15$ arcsec yr^{-1}. 21 VLM binaries were detected, 13 of them new discoveries. The new binary systems range in separation between 0.18 and 1.3 arcsec. The distance-corrected binary fraction is $13.6^{+6.5}_{-4}$ per cent, in agreement with previous results. Nine of the new binary systems have projected separations >10 au, including a new wide VLM binary with 27 au projected orbital separation. One of the new systems forms two components of a 2300 au separation triple system. We find that the projected separation distribution of the binaries with $V-K<6.5$ in this survey appears to be different from that of redder (lower mass) objects, suggesting a possible rapid change in the orbital radius distribution at around the M5 spectral type. The target sample was also selected to investigate X-ray activity among VLM binaries. There is no detectable correlation between excess X-ray emission and the frequency and binary properties of the VLM systems.

Key words: instrumentation: high angular resolution – methods: observational – techniques: high angular resolution – binaries: close – stars: low-mass, brown dwarfs.

1 INTRODUCTION

Multiple star systems offer a powerful way to constrain the processes of star formation. The distributions of companion masses, orbital radii and thus binding energies provide important clues to the systems' formation processes. In addition, binaries provide us with a method of directly determining the masses of the stars in the systems. This is fundamental to the calibration of the mass–luminosity relation (Henry & McCarthy 1993; Henry et al. 1999; Ségransan et al. 2000).

A number of recent studies have tested the stellar multiplicity fraction of low-mass and very low mass (VLM) stars. The fraction of known directly imaged companions to VLM stars is much lower than that of early M dwarfs and solar-type stars. Around 57 per cent of solar-type stars (F7–G9) have known stellar companions (Abt & Levy 1976; Duquennoy & Mayor 1991), while imaging and radial velocity surveys of early M dwarfs suggest that between 25 and 42 per cent have companions (Henry & McCarthy 1990; Fischer & Marcy 1992; Leinert et al. 1997; Reid & Gizis 1997). For M6–L1 primary spectral types direct imaging studies find binary fractions of only 10–20 per cent (Close et al. 2003; Siegler et al. 2005; Law, Hodgkin & Mackay 2006a; Montagnier et al. 2006), and similar binary fractions have been found for still later spectral types (Bouy et al. 2003; Burgasser et al. 2003; Gizis et al. 2003). Recent radial-velocity work has, however, suggested that a large fraction of apparently single VLM stars are actually very close doubles, and the VLM multiplicity fraction may thus be comparable to higher mass stars (Jeffries & Maxted 2005; Basri & Reiners 2006).

VLM M, L and T systems appear to have a tighter and closer distribution of orbital separations, peaking at around 4 au compared to 30 au for G dwarfs (Close et al. 2003). However, the relatively few known field VLM binaries limit the statistical analysis of the distribution, in particular for studying the frequency of the rare large orbital radii systems which offer strong constraints on some formation theories (e.g. Bate & Bonnell 2005; Phan-Bao et al. 2005; Law et al. 2006a; Artigau et al. 2007; Caballero 2007; Close et al. 2007).

We have been engaged in a programme to image a large and carefully selected sample of VLM stars, targeting separations greater than 1 au (Law et al. 2005, 2006a). The programme has yielded a total of 18 new VLM binary systems, where VLM is defined as a primary mass $<0.11\,M_{\odot}$. This paper presents the second of the surveys, targeting field stars in the range M4.5–M6.0. The spectral type range of this survey is designed to probe the transition between the properties of the 30 au median-radius binaries of the early M dwarfs and the 4 au median-radius of late M dwarf binaries.

⋆Based on observations made with the Nordic Optical Telescope, operated on the island of La Palma jointly by Denmark, Finland, Iceland, Norway and Sweden, in the Spanish Observatorio del Roque de los Muchachos of the Instituto de Astrofisica de Canarias.

†E-mail: nlaw@astro.caltech.edu

We observed 77 field M dwarf targets with estimated spectral types between M4.5 and M6.0, searching for companions with separations between 0.1 and 2.0 arcsec. The surveyed primary stellar masses range from 0.089 to 0.11 $M_\odot$ using the models in Baraffe et al. (1998).

It has been suggested in Makarov (2002) that F and G field stars detected in the *ROSAT* Bright Source Catalogue (BSC) are 2.4 times more likely to be members of wide (>0.3 arcsec) multiple systems than those not detected in X-rays. There is also a well-known correlation between activity and stellar rotation rates (e.g. Simon 1990; Soderblom et al. 1993; Terndrup et al. 2002). A correlation between binarity and rotation rate would thus be detectable as a correlation between activity and binarity. To test these ideas, we divided our targets into two approximately equal numbered samples on the basis of X-ray activity.

All observations used LuckyCam, the Cambridge Lucky Imaging system. The system has been demonstrated to reliably achieve diffraction-limited images in *I* band on 2.5-m telescopes (Baldwin et al. 2001; Tubbs et al. 2002; Mackay et al. 2004; Law, Mackay & Baldwin 2006b; Law 2007). A Lucky Imaging system takes many rapid short-exposure images, typically at 20–30 frames per second. The turbulence statistics are such that a high quality, near-diffraction-limited frame is recorded a few per cent of the time; in Lucky Imaging only those frames are aligned and co-added to produce a final high-resolution image. Lucky Imaging is an entirely passive process, and thus introduces no extra time overheads beyond those required for standard CCD camera observations. The system is thus very well suited to rapid high angular resolution surveys of large numbers of targets.

In Section 2 we describe the survey sample and the X-ray activity selection. Section 3 describes the observations and their sensitivity. Section 4 describes the properties of the 13 new VLM binaries, and Section 5 discusses the results.

2 THE SAMPLE

We selected a magnitude and colour limited sample of nearby late M dwarfs from the Lepine Shara Proper Motion (LSPM)-North high proper motion catalogue (Lépine & Shara 2005). The LSPM-North catalogue is a survey of the northern sky for stars with annual proper motions greater than 0.15 arcsec yr^{-1}. Most stars in the catalogue are listed with both Two Micron All Sky Survey (2MASS) infrared (IR) photometry and *V*-band magnitudes estimated from the photographic B_J and R_F bands.

The LSPM-North high proper motion cut ensures that all stars are relatively nearby, and thus removes contaminating distant giant stars from the sample. We cut the LSPM catalogue to include only stars with $V - K$ colour $\geqslant$6 and $\leqslant$7.5, and *K* magnitude brighter than 10. The colour cut selects approximately M4.5 to M6.0 stars; its effectiveness is confirmed in Law et al. (2006a).

2.1 X-ray selection

After the colour and magnitude cuts the sample contained 230 late M dwarfs. We then searched for evidence of X-ray emission from our targets. We mark a star as X-ray detected if the target star has a *ROSAT* All Sky Survey detection from the Faint Source Catalogue (Voges 2000) or the Bright Source Catalogue (Voges 1999) within 1.5 times the 1σ uncertainty in the X-ray position. Known or high-probability non-stellar X-ray associations noted in the quasars.org (QORG) catalogue of radio/X-ray sources (Flesch & Hardcastle 2004) are removed. Finally, we manually checked the Digitized Sky Survey (DSS) field around each star to remove those stars which did not show an unambiguous association with the position of the X-ray detection. The completeness and biases of the X-ray selection are discussed in Section 5.2.

One star in the sample, LSPM J0336+3118, is listed as a T Tauri in the SIMBAD data base, and was therefore removed from the sample. We note that in the case of the newly detected binary LSPM J0610+2234, which is $\sim 0.7\sigma$ away from the *ROSAT* X-ray source we associate with it, there is another bright star at 1.5σ distance which may be the source of the X-ray emission. GJ 376B is known to be a common proper motion (CPM) companion to the G star GJ 376, located at a distance of 134 arcsec (Gizis et al. 2000). Since the separation is very much greater than can detected in the LuckyCam survey, we treat it as a single star in the following analysis.

2.2 Target distributions

The cuts left 51 X-ray detected stars and 178 stars without *ROSAT* X-ray detections. We drew roughly equal numbers of stars at random from both of these lists to form the final observing target set of 37 X-ray detected stars and 40 non-X-ray-detected stars (described in Tables 1 and 2). For each star we detail the astrometry, photometry, estimated spectral type and the estimated fraction of the star's bolometric luminosity emitted in X-rays ($\log [L_x/L_{bol}]$). For the stars not detected by *ROSAT* we calculated an upper-limit X-ray flux on the basis of the *ROSAT* All Sky Survey exposure and background maps. We adopted a standard *ROSAT* counts per second to flux conversion factor of 6×10^{-12} erg cm^{-2} ct^{-1} (James et al. 2000). The stars' bolometric luminosities were estimated on the basis of 2MASS *K*-band photometry using the empirical relations in Leggett (1992) and Tinney, Mould & Reid (1993).

Two targets are found to have very large $\log(L_x/L_{bol})$ (GJ 376B and LSPM J1832+2030). Both are listed as flaring sources in Fuhrmeister & Schmitt (2003) and thus were probably observed during flare events (although Gizis et al. 2000 argues that GJ 376B is simply very active).

Four of the X-ray detected stars and four of the others were previously known to be binary systems and are detailed in Table 3. We reimaged them with LuckyCam to ensure a uniform survey sensitivity in both angular resolution and detectable companion contrast ratio.

Fig. 1 shows the survey targets' distributions in *K* magnitude, $V - K$ colour and photometrically estimated distance. Fig. 2 compares the targets to the rest of the stars in the LSPM catalogue. The X-ray and non-X-ray samples are very similar, although the non-X-ray sample has a slightly higher median distance, at 15.4 pc rather than 12.2 pc (the errors on the distance determination are about 30 per cent).

3 OBSERVATIONS

We imaged all 77 targets in a total of 11 h of on-sky time in 2005 June and November, using LuckyCam on the 2.56-m Nordic Optical Telescope. Each target was observed for 100 s in both i' and z' filters. Most of the observations were performed through varying cloud cover with a median extinction on the order of three magnitudes. This did not significantly affect the imaging performance, as all these stars are 3–4 mag brighter than the LuckyCam guide star requirements, but the sensitivity to faint objects was reduced and no calibrated photometry was attempted.

Table 1. The observed non-X-ray-detected sample. The quoted V and K magnitudes are taken from the LSPM catalogue. K magnitudes are based on 2MASS photometry; the LSPM-North V-band photometry is estimated from photographic B_J and R_F magnitudes and is thus approximate only, but is sufficient for spectral type estimation – see Section 4.2. Spectral types and distances are estimated from the V and K photometry (compared to SIMBAD spectral types) and the young-disc photometric parallax relations described in Leggett (1992). Spectral types have a precision of approximately 0.5 spectral classes and distances have a precision of ∼30 per cent. $\log (L_x/L_{bol})_{max}$ is estimated from the *ROSAT* FSC minimum detectable X-ray emission in that region and 2MASS photometry as described in the text.

LSPM ID	Other name	K	$V-K$	Est. SpT	PM arcsec yr^{-1}	$\log (L_x/L_{bol})_{max}$	LSPM ID	Other name	K	$V-K$	Est. SpT	PM arcsec yr^{-1}	$\log (L_x/L_{bol})_{max}$
LSPM J0023+7711	LHS 1066	9.11	6.06	M4.5	0.839	−3.7	LSPM J0711+4329	LHS 1901	9.13	6.74	M5.0	0.676	−3.4
LSPM J0035+0233		9.54	6.82	M5.0	0.299	−3.2	LSPM J0722+7305		9.44	6.20	M4.5	0.178	−3.4
LSPM J0259+3855	G134−63	9.52	6.21	M4.5	0.252	−3.4	LSPM J0736+0704	G89−32	7.28	6.01	M4.5	0.383	−4.1
LSPM J0330+5413		9.28	6.92	M5.0	0.151	−3.5	LSPM J0738+4925	LHS 5126	9.70	6.34	M4.5	0.497	−3.3
LSPM J0406+7916	G 248-12	9.19	6.43	M4.5	0.485	−3.4	LSPM J0738+1829		9.81	6.58	M5.0	0.186	−3.1
LSPM J0408+6910	G247−12	9.40	6.08	M4.5	0.290	−3.4	LSPM J0810+0109		9.74	6.10	M4.5	0.194	−3.2
LSPM J0409+0546		9.74	6.34	M4.5	0.255	−3.2	LSPM J0824+2555		9.70	6.10	M4.5	0.233	−3.3
LSPM J0412+3529		9.79	6.25	M4.5	0.184	−3.3	LSPM J0825+6902	LHS 246	9.16	6.47	M4.5	1.425	−3.5
LSPM J0414+8215	G222−2	9.36	6.13	M4.5	0.633	−3.4	LSPM J0829+2646	V* DX Cnc	7.26	7.48	M5.5	1.272	−4.1
LSPM J0417+0849		8.18	6.36	M4.5	0.405	−3.8	LSPM J0841+5929	LHS 252	8.67	6.51	M5.0	1.311	−3.7
LSPM J0420+8454		9.46	6.10	M4.5	0.279	−3.4	LSPM J0849+3936		9.64	6.25	M4.5	0.513	−3.2
LSPM J0422+3900		9.67	6.10	M4.5	0.840	−3.3	LSPM J0858+1945	V* EI Cnc	6.89	7.04	M5.5	0.864	−4.3
LSPM J0439+1615		9.19	7.05	M5.5	0.797	−3.4	LSPM J0859+2918	LP 312−51	9.84	6.26	M4.5	0.434	−3.1
LSPM J0501+2237		9.23	6.21	M4.5	0.248	−3.4	LSPM J0929+2558	LHS 269	9.96	6.67	M5.0	1.084	−3.1
LSPM J0503+2122	NLTT 14406	8.89	6.28	M4.5	0.177	−3.6	LSPM J0932+2659	GJ 354.1 B	9.47	6.33	M4.5	0.277	−3.4
LSPM J0546+0025	EM* RJHA 15	9.63	6.50	M4.5	0.309	−3.4	LSPM J0956+2239		8.72	6.06	M4.5	0.533	−3.7
LSPM J0602+4951	LHS 1809	8.44	6.20	M4.5	0.863	−3.7	LSPM J1848+0741		7.91	6.72	M5.0	0.447	−4.0
LSPM J0604+0741		9.78	6.15	M4.5	0.211	−3.3	LSPM J2215+6613		7.89	6.02	M4.5	0.208	−4.1
LSPM J0657+6219	GJ 3417	7.69	6.05	M4.5	0.611	−4.0	LSPM J2227+5741	NSV 14168	4.78	6.62	M5.0	0.899	−5.3
LSPM J0706+2624		9.95	6.26	M4.5	0.161	−3.0	LSPM J2308+0335		9.86	6.18	M4.5	0.281	−3.2

Table 2. The observed X-ray detected sample. The star properties are estimated as described in the caption to Table 1, with the exception of the use of the *ROSAT* FSC/BSC measured X-ray flux to derive log (L_x/L_{bol}). ST is the estimated spectral type; the *ROSAT* flux is given in units of counts per second.

LSPM ID	Other name	K	$V-K$	ST	PM arcsec yr^{-1}	*ROSAT* BSC/FSC ID	*ROSAT* CPS	log(L_x/L_{bol})
LSPM J0045+3347		9.31	6.50	M4.5	0.263	1RXS J004556.3+334718	2.522E-02	−3.3
LSPM J0115+4702S		9.31	6.04	M4.5	0.186	1RXS J011549.5+470159	4.323E-02	−3.1
LSPM J0200+1303		6.65	6.06	M4.5	2.088	1RXS J020012.5+130317	1.674E-01	−3.6
LSPM J0207+6417		8.99	6.25	M4.5	0.283	1RXS J020711.8+641711	8.783E-02	−2.9
LSPM J0227+5432		9.33	6.05	M4.5	0.167	1RXS J022716.4+543258	2.059E-02	−3.4
LSPM J0432+0006	LP 595−21	9.43	6.37	M4.5	0.183	1RXS J043256.1+000650	1.557E-02	−3.5
LSPM J0433+2044		8.96	6.47	M4.5	0.589	1RXS J043334.8+204437	9.016E-02	−2.9
LSPM J0610+2234		9.75	6.68	M5.0	0.166	1RXS J061022.8+223403	8.490E-02	−2.9
LSPM J0631+4129		8.81	6.34	M4.5	0.212	1RXS J063150.6+412948	4.275E-02	−3.0
LSPM J0813+7918	LHS 1993	9.13	6.07	M4.5	0.539	1RXS J081346.5+791822	1.404E-02	−3.7
LSPM J0921+4330	GJ 3554	8.49	6.21	M4.5	0.319	1RXS J092149.3+433019	3.240E-02	−3.5
LSPM J0953+2056	GJ 3571	8.33	6.15	M4.5	0.535	1RXS J095354.6+205636	2.356E-02	−3.7
LSPM J0958+0558		9.04	6.17	M4.5	0.197	1RXS J095856.7+055802	2.484E-02	−3.4
LSPM J1000+3155	GJ 376B	9.27	6.86	M5.0	0.523	1RXS J100050.9+315555	2.383E-01	−2.4
LSPM J1001+8109		9.41	6.20	M4.5	0.363	1RXS J100121.0+810931	3.321E-02	−3.2
LSPM J1002+4827		9.01	6.57	M5.0	0.426	1RXS J100249.7+482739	6.655E-02	−3.0
LSPM J1125+4319		9.47	6.16	M4.5	0.579	1RXS J112502.7+431941	5.058E-02	−3.0
LSPM J1214+0037		7.54	6.33	M4.5	0.994	1RXS J121417.5+003730	9.834E-02	−3.4
LSPM J1240+1955		9.69	6.08	M4.5	0.307	1RXS J124041.4+195509	2.895E-02	−3.1
LSPM J1300+0541		7.66	6.02	M4.5	0.959	1RXS J130034.2+054111	1.400E-01	−3.2
LSPM J1417+3142	LP 325−15	7.61	6.19	M4.5	0.606	1RXS J141703.1+314249	1.145E-01	−3.3
LSPM J1419+0254		9.07	6.29	M4.5	0.233	1RXS J141930.4+025430	2.689E-02	−3.4
LSPM J1422+2352	LP 381−49	9.65	6.38	M4.5	0.248	1RXS J142220.3+235241	2.999E-02	−3.1
LSPM J1549+7939	G256−25	8.86	6.11	M4.5	0.251	1RXS J154954.7+793949	2.033E-02	−3.6
LSPM J1555+3512	GJ 3928	8.04	6.02	M4.5	0.277	1RXS J155532.2+351207	1.555E-01	−3.0
LSPM J1640+6736	GJ 3971	8.95	6.91	M5.0	0.446	1RXS J164020.0+673612	7.059E-02	−3.0
LSPM J1650+2227		8.31	6.38	M4.5	0.396	1RXS J165057.5+222653	6.277E-02	−3.3
LSPM J1832+2030		9.76	6.28	M4.5	0.212	1RXS J183203.0+203050	1.634E-01	−2.3
LSPM J1842+1354		7.55	6.28	M4.5	0.347	1RXS J184244.9+135407	1.315E-01	−3.3
LSPM J1926+2426		8.73	6.37	M4.5	0.197	1RXS J192601.4+242618	1.938E-02	−3.7
LSPM J1953+4424	GJ 1245A	6.85	6.63	M5.0	0.624	1RXS J195354.7+442454	1.982E-01	−3.2
LSPM J2023+6710		9.17	6.60	M5.0	0.296	1RXS J202318.5+671012	2.561E-02	−3.4
LSPM J2059+5303	GSC 03952−01062	9.12	6.34	M4.5	0.170	1RXS J205921.6+530330	4.892E-02	−3.1
LSPM J2117+6402		9.18	6.62	M5.0	0.348	1RXS J211721.8+640241	3.628E-02	−3.2
LSPM J2322+7847		9.52	6.97	M5.0	0.227	1RXS J232250.1+784749	2.631E-02	−3.2
LSPM J2327+2710		9.42	6.07	M4.5	0.149	1RXS J232702.1+271039	4.356E-02	−3.0
LSPM J2341+4410		5.93	6.48	M4.5	1.588	1RXS J234155.0+441047	1.772E-01	−3.8

Table 3. The previously known binaries which were redetected by LuckyCam in this survey.

Name	Ref.
GJ 3417	Henry et al. (1999)
G89−32B	Henry et al. (1997)
V* EI Cnc	Gliese & Jahreiß (1991)
LP 595−21	Luyten (1997)
GJ 1245	McCarthy et al. (1988)
GJ 3928	McCarthy, Zuckerman & Becklin (2001)
LP 325−15	Delfosse et al. (1999)
LHS 1901	Montagnier et al. (2006)

3.1 Binary detection and photometry

Companions were detected according to the criteria described in detail in Law et al. (2006a). We required 10σ detections above both photon and speckle noise; the detections must appear in both i' and z' images. Detection is confirmed by comparison with point spread function (PSF) reference stars imaged before and after each target. In this case, because the observed binary fraction is only ∼30 per cent, other survey sample stars serve as PSF references. We measured resolved photometry of each binary system by the fitting and subtraction of two identical PSFs to each image, modelled as Moffat functions with an additional diffraction-limited core. In those cases where some aliasing is visible, leading to the appearance of an unphysical third component, we fit three identical PSFs and solved for the true binary flux ratio (Law 2007).

3.2 Sensitivity

The sensitivity of the survey was limited by the cloud cover. Because of the difficulty of flux calibration under very variable extinction conditions we do not give an overall survey sensitivity. However, a minimum sensitivity can be estimated. LuckyCam requires an $i' = +15.5$ m guide star to provide good correction; all stars in this survey must appear to be at least that bright during the observations.[1] The sensitivity of the survey around a $i = +15.5$ m star is calculated

[1] LSPM J2023+6710 was observed though ∼5 mag of cloud, much more than any other target in the survey, and was thus too faint for good performance Lucky Imaging. However, its bright companion is at 0.9 arcsec separation and so was easily detected.

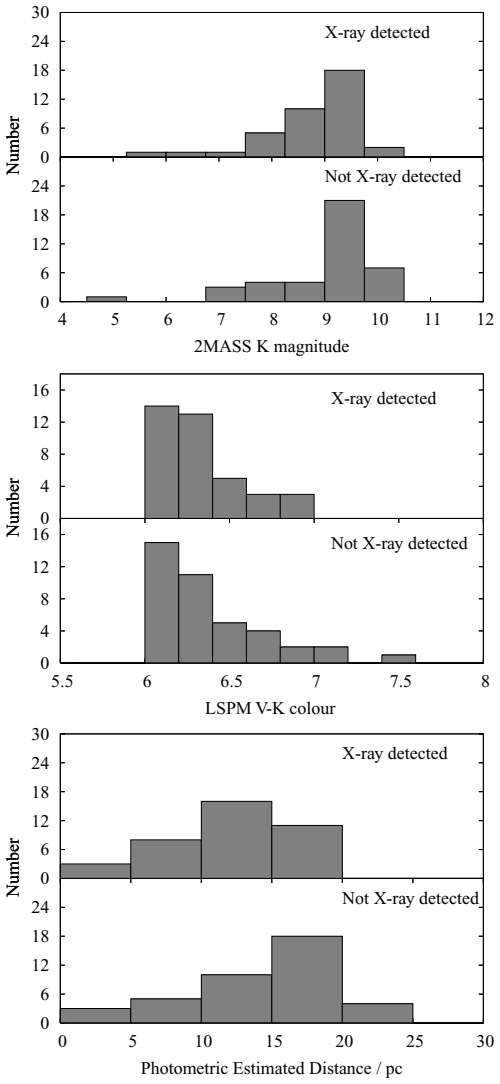

Figure 1. The 2MASS K magnitude, $V-K$ colour and distance distributions of the X-ray-active and non-X-ray-active samples. Distances are estimated from the LSPM $V-K$ colours of the samples and the $V-K$ photometric absolute magnitude relations detailed in Leggett (1992). The distances shown in this figure have a precision of approximately 30 per cent, and assume that all targets are single stars.

in Law et al. (2006a) and the sensitivity as a function of companion separation is discussed in Section 5.4.

The survey is also sensitive to white dwarf companions around all stars in the sample. However, until calibrated resolved photometry or spectroscopy is obtained for the systems it is not possible to distinguish between M dwarf and white dwarf companions. Since a large sample of very close M dwarf companions to white dwarf primaries have been found spectroscopically (for example Delfosse et al. 1999; Raymond et al. 2003), but very few have been resolved, it is unlikely that the companions are white dwarfs. It will, however, be of interest to further constrain the frequency of white dwarf and M dwarf systems.

4 RESULTS AND ANALYSIS

We found 13 new VLM binaries. The binaries are shown in Fig. 3 and the observed properties of the systems are detailed in Table 4.

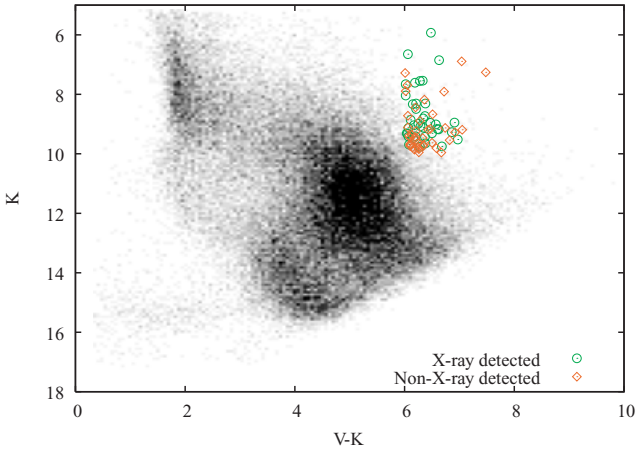

Figure 2. The observed samples, plotted in a K / $V-K$ colour–magnitude diagram. The background distribution shows all stars in the LSPM-North catalogue.

In addition to the new discoveries, we confirmed eight previously known binaries, detailed in Tables 3 and 4.

4.1 Confirmation of physical association

Seven of the newly discovered binaries have moved more than one DSS PSF radius between the acquisition of DSS images and these observations (Table 5). With a limiting magnitude of $i_N \sim +20.3$ m (Gal et al. 2004), the DSS images are deep enough for clear detection of all the companions found here, should they actually be stationary background objects. None of the DSS images show an object at the present position of the detected proposed companion, confirming the CPMs of these companions with their primaries.

The other binaries require a probabilistic assessment. In the entire LuckyCam VLM binary survey, covering a total area of (22 × 14.4 arcsec^2) × 122 fields, there are 10 objects which would have been detected as companions if they had happened to be close to the target star. One of the detected objects is a known wide CPM companion; others are due to random alignments. For the purposes of this calculation, we assume that all detected widely separated objects are not physically associated with the target stars.

Limiting the detection radius to 2 arcsec around the target star (we confirm wider binaries by testing for CPM against DSS images) 0.026 random alignments would be expected in our data set. This corresponds to a probability of only 2.5 per cent that one or more of the apparent binaries detected here is a chance alignment of the stars. We thus conclude that all the detected binaries are physically associated systems.

4.2 Constraints on the nature of the target stars

Clouds unfortunately prevented calibrated resolved photometry for the VLM systems. However, unresolved V- and K-band photometry listed in the LSPM survey gives useful constraints on the spectral types of these targets. About one third of the sample has a listed spectral type in the SIMBAD data base (from Jaschek 1978). To obtain estimated spectral types for the VLM binary systems, we fit the LSPM $V-K$ colours to those spectral types. The fit has a 1σ

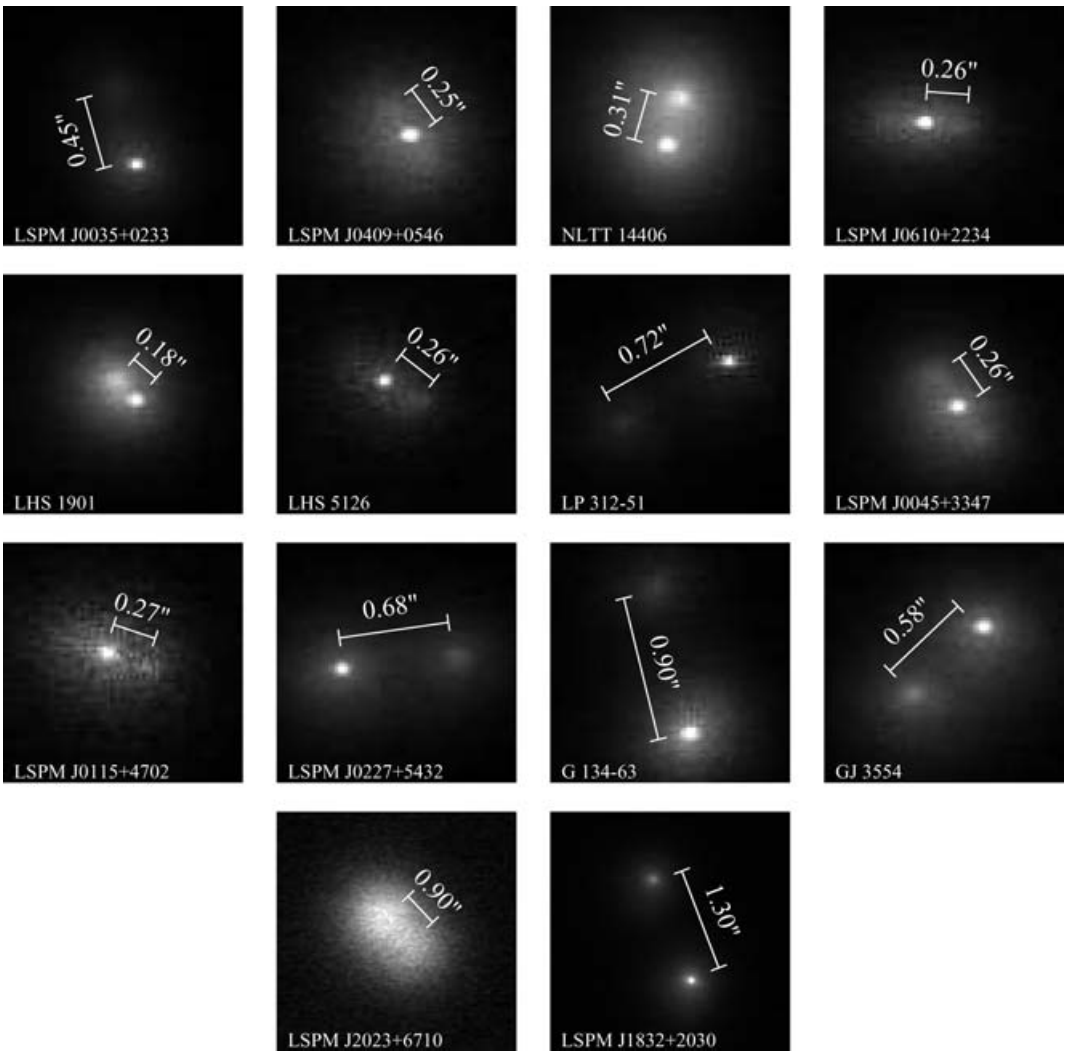

Figure 3. The newly discovered binaries. All images are orientated with north up and east to the left. The images are the results of a Lucky Imaging selection of the best 10 per cent of the frames taken in i', with the following exceptions: LSPM J0409+0546, LSPM J0610+2234 and LP 312−51 are presented in the z' band, as the cloud extinction was very large during their i' observations. The image of LHS 5126 uses the best 2 per cent of the frames taken and LSPM J0115+4702S uses the best 1 per cent, to improve the light concentration of the secondary. LSPM J2023+6710 was observed through more than 5 mag of cloud extinction, and was thus too faint for Lucky Imaging; a summed image with each frame centroid-centred is presented here, showing clear binarity. LHS 1901 was independently found by Montagnier et al. (2006) during a similar M dwarf survey. We present our image here to confirm its binarity.

uncertainty of ∼0.5 spectral types. The colour–magnitude relations in Leggett (1992) show the unresolved system colour is dominated by the primary for all M2–M9 combinations of primary and secondary. We then estimate the secondaries' spectral types by (1) assuming the estimated primary spectral type to be the true value and (2) using the spectral type versus i' and z' absolute magnitude relations in Hawley et al. (2002) to estimate the difference in spectral types between the primary and secondary. This procedure gives useful constraints on the nature of the systems, although resolved spectroscopy is required for definitive determinations.

4.3 Distances

The measurement of the distances to the detected binaries is a vital step in the determination of the orbital radii of the systems. None of the newly discovered binaries presented here has a measured parallax (although four[2] of the previously known systems do) and calibrated resolved photometry is not available for almost all the systems. We therefore calculate distances to the newly discovered systems using the $V - K$ colour–absolute magnitude relations

[2] G132−25 (NLTT 2511) is listed in Reid & Cruz (2002) and the SIMBAD data base as having a trigonometric parallax of 14.7 ± 4.0 mas, based on the Yale General Catalogue of Trigonometric Stellar Parallaxes (van Altena et al. 2001). However, this appears to be a misidentification, as the star is not listed in the Yale Catalogue. The closest star listed, which does have the parallax stated for G132−25 in Reid & Cruz (2002), is LP 294−2 (NLTT 2532). This star has a very different proper motion speed and direction to G132−25 (0.886 arcsec yr^{-1} versus 0.258 arcsec yr^{-1} in the LSPM catalogue and SIMBAD). In addition, the G132−25 LSPM V and K photometry is inconsistent with that of an M dwarf at a distance of 68 pc. We thus do not use the stated parallax for G132−25.

Table 4. The observed properties of the detected binaries. The top group are stars with newly detected companions; the bottom group are the previously known systems. LSPM J0409+0546 and J0610+2234 were observed though thick cloud and in poor seeing, and so only upper limits on the contrast ratio are given. LSPM J2023+6710 was not observed in z', and cloud prevented useful z' observations of LSPM J0035+0233.

Name	$\Delta\, i'$	$\Delta\, z'$	Sep. (arcsec)	PA (°)	Epoch	X-ray emitter?
LSPM J0035+0233	1.30 ± 0.30		0.446 ± 0.01	14.3 ± 1.4	2005.9	
LSPM J0409+0546	<1.5	<1.5	0.247 ± 0.01	40.0 ± 3.2	2005.9	
NLTT 14406	1.30 ± 0.30	0.77 ± 0.30	0.310 ± 0.01	351.6 ± 1.1	2005.9	
LSPM J0610+2234	<1.0	<1.0	0.255 ± 0.01	268.4 ± 2.7	2005.9	*
LHS 5126	0.50 ± 0.20	0.50 ± 0.30	0.256 ± 0.02	235.1 ± 3.4	2005.9	
LP 312−51	0.74 ± 0.10	0.51 ± 0.10	0.716 ± 0.01	120.5 ± 1.1	2005.9	
LSPM J0045+3347	0.80 ± 0.35	0.77 ± 0.35	0.262 ± 0.01	37.6 ± 1.9	2005.9	*
LSPM J0115+4702S	0.55 ± 0.25	0.73 ± 0.25	0.272 ± 0.01	249.8 ± 1.3	2005.9	*
LSPM J0227+5432	0.60 ± 0.10	0.59 ± 0.10	0.677 ± 0.01	275.8 ± 1.1	2005.9	*
G134−63	1.55 ± 0.10	1.35 ± 0.10	0.897 ± 0.01	13.6 ± 1.1	2005.9	
GJ 3554	0.51 ± 0.20	0.57 ± 0.20	0.579 ± 0.01	44.0 ± 1.1	2005.9	*
LSPM J2023+6710	0.55 ± 0.20		0.900 ± 0.15	232.5 ± 3.2	2005.9	*
LSPM J1832+2030	0.48 ± 0.10	0.45 ± 0.10	1.303 ± 0.01	20.6 ± 1.1	2005.4	*
GJ 3417	1.66 ± 0.10	1.42 ± 0.10	1.526 ± 0.01	-39.8 ± 1.0	2005.9	
LHS 1901	1.30 ± 0.70	1.30 ± 0.70	0.177 ± 0.01	51.4 ± 1.6	2005.9	
G89−32	0.43 ± 0.10	0.38 ± 0.10	0.898 ± 0.01	61.3 ± 1.0	2005.9	
V* EI Cnc	0.62 ± 0.10	0.49 ± 0.10	1.391 ± 0.01	76.6 ± 1.0	2005.9	
LP 595−21	0.74 ± 0.10	0.60 ± 0.10	4.664 ± 0.01	80.9 ± 1.0	2005.9	*
GJ 1245AC	2.95 ± 0.20	2.16 ± 0.20	1.010 ± 0.01	-11.3 ± 1.0	2005.4	*
GJ 3928	2.32 ± 0.20	2.21 ± 0.20	1.556 ± 0.01	-10.7 ± 1.0	2005.4	*
LP 325−15	0.36 ± 0.10	0.33 ± 0.10	0.694 ± 0.01	-21.5 ± 1.0	2005.4	*

Table 5. The newly discovered binaries which have moved far enough since DSS observations to allow confirmation of the CPM of their companions.

LSPM ID	Years since DSS obs.	Dist. moved
1RXS J004556.3+334718	16.2	4.3 arcsec
G134−63	16.2	4.1 arcsec
NLTT 14406	19.1	3.4 arcsec
LHS 5126	6.8	3.4 arcsec
LP 312−51	7.6	3.3 arcsec
GJ 3554	15.8	5.0 arcsec
LSPM J2023+6710	14.2	4.2 arcsec

described in Leggett (1992). Calculation of the distances in this manner requires care, as the *V*- and *K*-band photometry is unresolved, and so two luminous bodies contribute to the observed colours and magnitudes.

The estimated distances to the systems, and the resulting projected separations, are given in Table 6. The stated 1σ distance ranges include the following contributions.

(i) A 0.6 mag Gaussian-distributed uncertainty in the $V - K$ colour of the system (a combination of the colour uncertainty noted in the LSPM catalogue and the maximum change in the $V - K$ colour of the primary induced by a close companion).

(ii) A 0.3 mag Gaussian-distributed uncertainty in the absolute *K*-band magnitude of the system, from the uncertainty in the colour–absolute magnitude relations from Leggett (1992).

(iii) A 0.75 mag flat-distributed uncertainty in the absolute *K*-band magnitude of the system, to account for the unknown *K*-band contrast ratio of the binary system.

The resulting distances have 1σ errors of approximately 35 per cent, with a tail towards larger distances due to the *K*-band contrast ratio uncertainties.

4.4 NLTT 14406 – a newly discovered triple system

We found NLTT 14406 to have a 0.31 arcsec separation companion. NLTT 14406 is identified with LP 359−186 in the NLTT catalogue (Luyten 1995), although it is not listed in the revised NLTT catalogue (Salim & Gould 2003). LP 359−186 is a component of the CPM binary LDS 6160 (Luyten 1997), with the primary being LP 359−216 (NLTT 14412), 167-arcsec distant and listed in the SIMBAD data base as a M2.5 dwarf.

The identification of these high proper motion stars can be occasionally problematic when working over long time baselines. As a confirmatory check, the LSPM-listed proper motion speeds and directions of these candidate CPM stars agree to within 1σ (using the stated LSPM proper motion errors).

In the LSPM catalogue, the two stars are separated by 166.3 arcsec at the J2000.0 epoch. We thus identify our newly discovered 4.4 au separation companion to NLTT 14406 as a member of a triple system with an M2.5 primary located at 2280^{1080}_{-420} au separation.

5 DISCUSSION

5.1 The binary frequency of stars in this survey

We detected 13 new binaries in a sample of 77 VLM stars, as well as a further eight previously known binaries. This corresponds to a binary fraction of $27.2^{+5.6}_{-4.4}$ per cent, assuming Poisson errors. However, the binaries in our sample are brighter on average than single stars of the same colour and so were selected from a larger volume. Correcting for this, assuming a range of contrast ratio distributions between all binaries being equal magnitude and all contrast ratios being equally likely (Burgasser et al. 2003), we find a distance-corrected binary fraction of $13.6^{+6.5}_{-4}$ per cent.

However, because the binaries are more distant on average than the single stars in this survey, they also have a lower average proper

Table 6. The derived properties of the binary systems. The top group are stars with newly detected companions; the bottom group are the previously known binaries. All parallaxes are from the Yale General Catalogue of Trigonometric Stellar Parallaxes (van Altena, Lee & Hoffleit 2001). Distances and projected separations are estimated as noted in the text; the stated errors are 1σ. The primaries' spectral types have a 1σ uncertainty of $\sim$0.5 subtypes (Section 4.2); the difference in spectral types is accurate to $\sim$0.5 spectral subtypes.

Name	Parallax (mas)	Distance (pc)	Proj. sep. (au)	Prim. ST (est.)	Sec. ST (est.)
LSPM J0035+0233	···	$14.5^{+6.3}_{-2.4}$	$6.8^{+3.1}_{-1.0}$	M5.0	M6.0
LSPM J0409+0546	···	$19.9^{+9.1}_{-3.8}$	$4.9^{+2.7}_{-0.7}$	M4.5	$\leqslant$M6.0
NLTT 14406	···	$13.7^{+6.5}_{-2.5}$	$4.4^{+2.3}_{-0.7}$	M4.5	M5.5
LSPM J0610+2234	···	$17.0^{+7.5}_{-2.9}$	$4.6^{+2.1}_{-0.8}$	M5.0	$\leqslant$M6.0
LHS 5126	···	$19.5^{+8.9}_{-3.7}$	$4.9^{+2.9}_{-0.6}$	M4.5	M5.0
LP 312−51	···	$21.5^{+10.1}_{-4.0}$	$16.1^{+8.2}_{-2.7}$	M4.5	M5.0
LSPM J0045+3347	···	$14.9^{+7.0}_{-2.6}$	$4.0^{+2.1}_{-0.6}$	M4.5	M5.5
LSPM J0115+4702S	···	$18.7^{+9.3}_{-3.6}$	$5.2^{+2.9}_{-0.9}$	M4.5	M5.0
LSPM J0227+5432	···	$18.6^{+9.5}_{-3.4}$	$13.2^{+7.2}_{-2.2}$	M4.5	M5.0
G134−63	···	$18.8^{+9.3}_{-3.4}$	$17.6^{+9.4}_{-2.8}$	M4.5	M5.5
GJ 3554	···	$11.8^{+5.6}_{-2.2}$	$7.1^{+3.7}_{-1.2}$	M4.5	M4.5
LSPM J2023+6710	···	$13.6^{+5.9}_{-2.5}$	$12.8^{+6.5}_{-2.6}$	M5.0	M5.0
LSPM J1832+2030	···	$20.6^{+9.6}_{-3.9}$	$27.0^{+14.6}_{-4.0}$	M4.5	M5.0
GJ 3417	87.4 ± 2.3	$11.4^{+0.3}_{-0.3}$	$17.5^{+0.5}_{-0.5}$	M4.5	M6.5
LHS 1901	···	$12.3^{+5.6}_{-2.0}$	$2.3^{+1.1}_{-0.4}$	M4.5	M6.0
G89−32	···	$7.3^{+3.9}_{-1.3}$	$6.5^{+3.5}_{-1.1}$	M4.5	M5.0
V* EI Cnc	191.2 ± 2.5	$5.23^{+0.07}_{-0.07}$	$7.27^{+0.11}_{-0.11}$	M5.5	M6.0
LP 595−21	···	$16.5^{+8.2}_{-2.7}$	$76.2^{+38.7}_{-11.8}$	M4.5	M5.5
GJ 1245AC	220.2 ± 1.0	$4.54^{+0.02}_{-0.02}$	$4.6^{+0.05}_{-0.05}$	M5.0	M8.5
GJ 3928	···	$10.2^{+5.6}_{-1.7}$	$15.7^{+8.8}_{-2.5}$	M4.5	M6.5
LP 325−15	62.2 ± 13.0	$16.1^{+3.4}_{-3.4}$	$11.2^{+2.4}_{-2.4}$	M4.5	M4.5

motion. The LSPM proper motion cut will thus preferentially remove binaries from a sample which is purely selected on magnitude and colour. The above correction factor for the increased magnitude of binary systems does not include this effect, and so will underestimate the true binary fraction of the survey.

5.2 Biases in the X-ray sample

Before testing for correlations between X-ray emission and binary parameters, it is important to assess the biases introduced in the determination of the X-ray detected star's emission. The X-ray flux assignment criteria described in Section 2.1 are conservative. To reduce false associations, the X-ray source must appear within 1.5σ of the candidate star, which implies that $\sim$13 per cent of true associations are rejected. The requirement for an unambiguous association will also reject some fraction of actual X-ray emitters (10 per cent of the candidate emitting systems were rejected on this basis). The non-X-ray-detected sample will thus contain some systems that do actually meet the X-ray flux-emitting limit and so have underestimated upper-limit fluxes.

The X-ray source detection itself, which cuts only on the detection limit in the *ROSAT* Faint Source Catalogue (FSC), is biased both towards some sky regions (the *ROSAT* All Sky Survey does not have uniform exposure time; Voges 1999) and towards closer stars. However, the distance bias can be effectively removed by the use of the distance-independent estimator of X-ray emission $\log(L_{\rm x}/L_{\rm bol})$, while the sky-position bias is unimportant for our field-star sample.

Finally, the X-ray active stars in our sample represent a different stellar population from the less-active stars. In particular, the X-ray active stars are more likely to be young (e.g. Jeffries 1999, and references therein). It may thus be difficult to disentangle the biases introduced by selecting young stars from those intrinsic to the population of X-ray emitting older stars. As the results below show, there are no detectable correlations between binarity and X-ray emission. If correlations are detected in larger samples, constraints on the ages of the targets would have to be found to investigate the causes of the correlations.

5.3 Is X-ray activity an indicator of binarity?

11 of the 21 detected binaries have detected *ROSAT* X-ray fluxes. The average $\log(L_{\rm x}/L_{\rm bol})$ of the binaries with known X-ray flux is -3.19 ± 0.15, while the average for the single stars is -3.24 ± 0.09 (Fig. 4). If the two possible flaring sources are omitted the X-ray luminosity fractions are -3.27 ± 0.15 and -3.28 ± 0.10, respectively. We therefore conclude that binarity does not appear to be correlated with excess X-ray emission.

This contrasts with the 2.4 times higher binarity among the similarly selected sample of F and G type X-ray active stars in Makarov (2002). Since the fraction of stars showing X-ray activity increases towards later types, it is possible that the Makarov sample preferentially selects systems containing an X-ray emitting late M dwarf. However, most of the stellar components detected in Makarov (2002) are F and G types.

The much longer spin-down time-scales of late M dwarfs, in combination with the rotation-activity paradigm, may explain the lack of activity–binarity correlation in late M dwarfs. Delfosse et al. (1998) show that young disc M dwarfs with spectral types later than

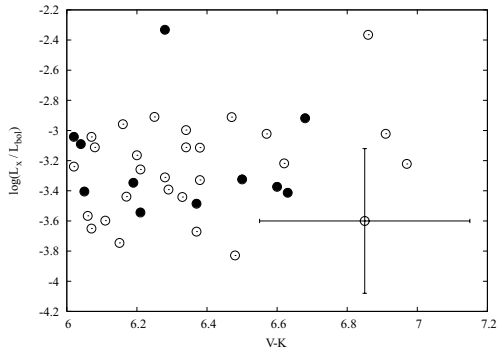

Figure 4. The fraction of stellar luminosity which appears as X-ray emission. Empty circles denote single stars; filled circles denote the binaries detected in this survey. A point is added to show typical error bars. No binarity correction is made to either the X-ray flux or K magnitude. The two high points are likely due to flaring.

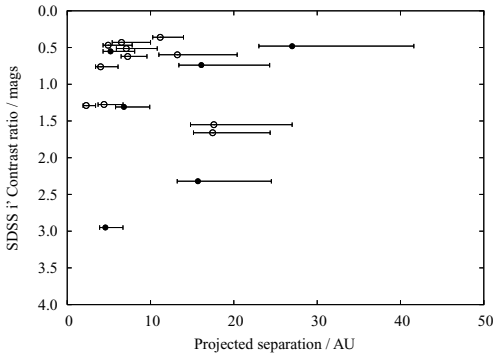

Figure 5. The i-band contrast ratios of the detected binaries, plotted as a function of binary separation in au. For reasons of clarity, the 76-au binary and the contrast ratio error bars (Table 4) have been omitted. Filled circles are targets where log (L_x/L_{bol}) or the upper limit log $(L_x/L_{bol})_{max}$ exceeds -3.27, the average measured log (L_x/L_{bol}) in our survey.

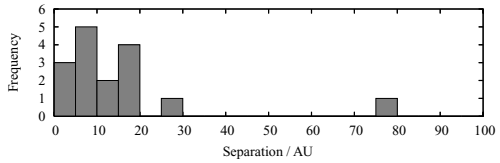

Figure 6. The histogram distribution of projected separations of the detected binaries in the sample.

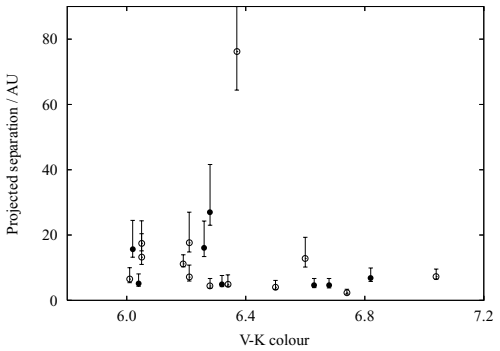

Figure 7. Projected separations in the detected binaries as a function of colour. $V-K=6$ corresponds approximately to M4.5, and $V-K=7$ to M5.5. Filled circles are X-ray emitters. For clarity, the $\sim$0.3 mag horizontal error bars have been omitted. Filled circles are targets where $\log(L_x/L_{bol})$ or the upper limit $\log(L_x/L_{bol})_{max}$ exceeds the average measured $\log(L_x/L_{bol})$ in our survey. There is no obvious correlation between X-ray emission and projected separation.

around M3 are still relatively rapidly rotating (with $v \sin i$s up to 40 km s^{-1} and even 60 km s^{-1} in one case), while earlier spectral types do not have detectable rotation periods to the limit of their sensitivity (around 2 km s^{-1}). Indeed solar type stars spin-down on relatively short time-scales, for example in the 200-Myr-old open cluster M34 Irwin et al. (2006) find that the majority of solar type stars have spun-down to periods of around 7 d ($V_{rot} \sim 7$ km s^{-1}). The M dwarfs thus have a high probability of fast rotation and thus activity even when single, which could washout any obvious binarity correlation with X-ray activity.

5.4 Contrast ratios

In common with previous surveys, the new systems have low contrast ratios. All but two of the detected systems have contrast ratios <1.7 mag. This is well above the survey sensitivity limits, as illustrated by the two binaries detected at much larger contrast ratios. Although those two systems are at larger radii, they would have been detected around most targets in the survey at as close as 0.2–0.3 arcsec.

It is difficult to obtain good constraints on the mass contrast ratio for these systems because of the lack of calibrated photometry, and so we leave the determination of the individual component masses for future work. However, we note that an interesting feature of the sample is that no binaries with contrast ratios consistent with equal-mass stars are detected.

There is no obvious correlation between the projected separation and the i-band contrast ratios nor between X-ray emission and the contrast ratios (Fig. 5).

5.5 The distribution of projected separations

Early M dwarf and G dwarf binaries have a broad orbital radius peak of around 30 au (Duquennoy & Mayor 1991; Fischer & Marcy 1992), while late M dwarfs have a peak at around 4 au (e.g. Close et al. 2005). Our survey covers a narrow (0.02 $M_\odot$) mass range in the region between the two populations and so allows us to test the rapidity of the transition in binary properties.

The projected separation distribution derived in this survey (Fig. 6) replicates the previously known VLM star 4 au orbital radius peak. However, nine of the 21 systems are at a projected separation of more than 10 au and most of these have relatively blue colours (Fig. 7). These wide VLM binaries are rare – in the 36 M6–M7.5 M dwarf sample of Siegler et al. (2005), five binaries are detected but none is found to be wider than 10 au.

Could the difference in detected projected separations be due to differing sensitivities to close companions? This is unlikely for a number of reasons. First, the Siegler et al. (2005) survey is sensitive to separations down to 0.1 arcsec, a value very similar to the minimum detectable separation of almost all our targets.[3] Secondly,

[3] Almost all of our observations reached the 0.08 arcsec diffraction-limited resolution of the 2.5-m telescope. A small number (5–10) had somewhat lower resolution, down to 0.2 arcsec. Only one of our observations (LSPM 2023+6710) was significantly poorer resolution.

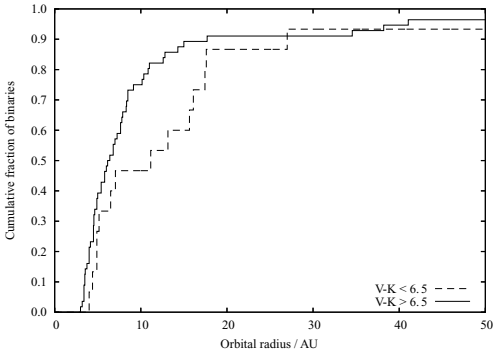

Figure 8. The cumulative distribution of projected separation of the detected binaries in the sample with $V - K < 6.5$ (dashed line). The solid line shows those with $V - K > 6.5$, with the addition of the full sample of known VLM binaries with total system masses $<0.2\,M_{\odot}$. Neither distribution reaches a fraction of 1.0 because of a small number of binaries wider than 50 au.

the Siegler sample is certainly sensitive to the wide binaries we detected. If the two surveys probe the same population Siegler et al. (2005) would be expected to find 4±2 binaries wider than 10 au in their 36 star sample. Finally, the raw and distance-corrected binary fractions are very similar in the two surveys, suggesting that the difference in the distributions is unlikely to be simply because our survey is missing a population of close companions.

To test for a rapid transition between the low-mass and VLM binary properties in the mass range covered by our survey, we supplemented the $V - K > 6.5$ systems from the LuckyCam sample with the known VLM binaries from the Very Low Mass Binaries Archive[4] (which, due to a different mass cut, all have a lower system mass than the LuckyCam sample). To reduce selection effects from the instrumental resolution cut-offs we only considered VLM binaries with projected separations >3.0 au.

The resulting cumulative probability distributions are shown in Fig. 8. There is a deficit in wider systems in the redder sample compared to the more massive, bluer systems. A K–S test between the two projected separation distributions gives an 8 per cent probability that they are derived from the same underlying distribution. This suggests a possibly rapid change in the incidence of systems with projected separations >10 au, at around the M5–M5.5 spectral type. However, confirmation of the rapid change will require a larger number of binaries and a more precise mass determination for each system.

5.6 The LuckyCam surveys in the context of formation mechanisms

VLM star formation is currently usually modelled as fragmentation of the initial molecular cloud core followed by ejection of the low-mass stellar embryos before mass accretion has completed – the ejection hypothesis (Reipurth & Clarke 2001). Multiple systems formed by fragmentation are limited to be no smaller than 10 au by the opacity limit (e.g. Boss 1988), although closer binaries can be formed by dynamical interactions and orbital decay (Bate, Bonnell & Bromm 2002).

The ejection hypothesis predicted binary frequency is about 8 per cent (Bate & Bonnell 2005); few very close (<3 au) binaries are expected (Umbreit et al. 2005) without appealing to orbital decay. Few wide binaries with low binding energies are expected to survive the ejection, although recent models produce some systems wider than 20 au when two stars are ejected simultaneously in the same direction (Bate & Bonnell 2005). The standard ejection hypothesis orbital radius distribution is thus rather tight and centred at about 3–5 au, although its width can be enlarged by appealing to the above additional effects.

The LuckyCam VLM binary surveys (this work and Law et al. 2006a) found several wide binary systems, with 11 of the 24 detected systems at more than 10 au projected separation and three at more than 20 au. With the latest models, the ejection hypothesis cannot be ruled out by these observations, and indeed (as suggested in Bate & Bonnell 2005) the frequency of wider systems will be very useful for constraining more sophisticated models capable of predicting the frequency in detail. The observed distance-bias-corrected binary frequency in the LuckyCam survey is consistent with the ejection hypothesis models, but may be inconsistent when the number of very close binaries undetected in the surveys is taken into account (Jeffries & Maxted 2005; Maxted & Jeffries 2005).

For fragmentation to reproduce the observed projected separation distribution, including the likely number of very close systems, dynamical interactions and orbital decay must be very important processes. However, smoothed particle hydrodynamics (SPH) models also predict very low numbers of close binaries. An alternate mechanism for the production of the closest binaries is thus required (Jeffries & Maxted 2005), as well as modelling constraints to test against the observed numbers of wider binaries. Radial velocity observations of the LuckyCam samples to search for much closer systems would offer a very useful insight into the full orbital radius distribution that must be reproduced by the models.

6 CONCLUSIONS

We found 21 VLM binary systems in a 77 star sample, including one binary in a 2300-au-wide triple system with a higher mass primary and one VLM system with a 27 au projected separation. 13 of the binary systems are new discoveries. All of the new systems are significantly fainter than the previously known close systems in the sample. The distance-corrected binary fraction is $13.6^{+6.5}_{-4}$ per cent, in agreement with previous results. There is no detectable correlation between X-ray emission and binarity. The projected separation distribution of the binaries appears to show characteristics of both the late and early M dwarf distributions, with nine systems having a projected separation of more than 10 au. We find that the projected separation distribution of the binaries with $V - K < 6.5$ in this survey appears to be inconsistent with that of lower mass objects, suggesting a possible sharp cut-off in the number of binaries wider than 10 au at about the M5 spectral type.

ACKNOWLEDGMENTS

The authors would like to particularly thank the staff members at the Nordic Optical Telescope. They would also like to thank John Baldwin and Peter Warner for many helpful discussions. An anonymous referee gave suggestions which significantly strengthened the paper. NML acknowledges support from the UK Particle Physics and Astronomy Research Council (PPARC). This research has made use of the SIMBAD data base, operated at CDS, Strasbourg, France. It also made use of NASA's Astrophysics Data System Bibliographic Services.

[4] Collated by Nick Siegler; VLM there is defined at the slightly lower cut-off of total system mass of $<0.2\,M_{\odot}$.

REFERENCES

Abt H. A., Levy S. G., 1976, ApJS, 30, 273
Artigau É., Lafrenière D., Doyon R., Albert L., Nadeau D., Robert J., 2007, ApJ, 659, L49
Baldwin J. E., Tubbs R. N., Cox G. C., Mackay C. D., Wilson R. W., Andersen M. I., 2001, A&A, 368, L1
Baraffe I., Chabrier G., Allard F., Hauschildt P. H., 1998, A&A, 337, 403
Basri G., Reiners A., 2006, AJ, 132, 663
Bate M. R., Bonnell I. A., 2005, MNRAS, 356, 1201
Bate M. R., Bonnell I. A., Bromm V., 2002, MNRAS, 336, 705
Boss A. P., 1988, ApJ, 331, 370
Bouy H., Brandner W., Martín E. L., Delfosse X., Allard F., Basri G., 2003, AJ, 126, 1526
Burgasser A. J., Kirkpatrick J. D., Reid I. N., Brown M. E., Miskey C. L., Gizis J. E., 2003, ApJ, 586, 512
Caballero J. A., 2007, A&A, 462, L61
Close L. M., Siegler N., Freed M., Biller B., 2003, ApJ, 587, 407
Close L. M. et al., 2005, Nat, 433, 286
Close L. M. et al., 2007, ApJ, 660, 1492
Delfosse X., Forveille T., Perrier C., Mayor M., 1998, A&A, 331, 581
Delfosse X., Forveille T., Beuzit J.-L., Udry S., Mayor M., Perrier C., 1999, A&A, 344, 897
Duquennoy A., Mayor M., 1991, A&A, 248, 485
Fischer D. A., Marcy G. W., 1992, ApJ, 396, 178
Flesch E., Hardcastle M. J., 2004, A&A, 427, 387
Fuhrmeister B., Schmitt J. H. M. M., 2003, A&A, 403, 247
Gal R. R., de Carvalho R. R., Odewahn S. C., Djorgovski S. G., Mahabal A., Brunner R. J., Lopes P. A. A., 2004, AJ, 128, 3082
Gizis J. E., Monet D. G., Reid I. N., Kirkpatrick J. D., Burgasser A. J., 2000, MNRAS, 311, 385
Gizis J. E., Reid I. N., Knapp G. R., Liebert J., Kirkpatrick J. D., Koerner D. W., Burgasser A. J., 2003, AJ, 125, 3302
Gliese W., Jahreiß H., 1991, Technical Report, Preliminary Version of the Third Catalogue of Nearby Stars
Hawley S. L. et al., 2002, AJ, 123, 3409
Henry T. J., McCarthy D. W., 1990, ApJ, 350, 334
Henry T. J., McCarthy D. W., 1993, AJ, 106, 773
Henry T. J., Ianna P. A., Kirkpatrick J. D., Jahreiss H., 1997, AJ, 114, 388
Henry T. J., Franz O. G., Wasserman L. H., Benedict G. F., Shelus P. J., Ianna P. A., Kirkpatrick J. D., McCarthy D. W., 1999, ApJ, 512, 864
Irwin J., Aigrain S., Hodgkin S., Irwin M., Bouvier J., Clarke C., Hebb L., Moraux E., 2006, MNRAS, 370, 954
James D. J., Jardine M. M., Jeffries R. D., Randich S., Collier Cameron A., Ferreira M., 2000, MNRAS, 318, 1217
Jaschek M., 1978, Bull. Inf. Cent. Donnees Stellaires, 15, 121
Jeffries R. D., 1999, in Butler C. J., Doyle J. G., eds, ASP Conf. Ser. Vol. 158, Solar and Stellar Activity: Similarities and Differences X-Rays from Open Clusters. Astron. Soc. Pac., San Francisco, p. 75
Jeffries R. D., Maxted P. F. L., 2005, Astron. Nachr., 326, 944
Law N. M., 2007, Observatory, 127, 71
Law N. M., Hodgkin S. T., Mackay C. D., Baldwin J. E., 2005, Astron. Nachr., 326, 1024
Law N. M., Hodgkin S. T., Mackay C. D., 2006a, MNRAS, 368, 1917L
Law N. M., Mackay C. D., Baldwin J. E., 2006b, A&A, 446, 739
Leggett S. K., 1992, ApJS, 82, 351
Leinert C., Henry T., Glindemann A., McCarthy D. W., 1997, A&A, 325, 159
Lépine S., Shara M. M., 2005, AJ, 129, 1483
Luyten W. J., 1995, VizieR Online Data Catalog, 1098, 0
Luyten W. J., 1997, VizieR Online Data Catalog, 1130, 0
McCarthy D. W., Henry T. J., Fleming T. A., Saffer R. A., Liebert J., Christou J. C., 1988, ApJ, 333, 943
McCarthy C., Zuckerman B., Becklin E. E., 2001, AJ, 121, 3259
Mackay C. D., Baldwin J., Law N., Warner P., 2004, Proc. SPIE, 5492, 128
Makarov V. V., 2002, ApJ, 576, L61
Maxted P. F. L., Jeffries R. D., 2005, MNRAS, 362, L45
Montagnier G. et al., 2006, A&A, 460, L19
Phan-Bao N., Martín E. L., Reylé C., Forveille T., Lim J., 2005, A&A, 439, L19
Raymond S. N. et al., 2003, AJ, 125, 2621
Reid I. N., Cruz K. L., 2002, AJ, 123, 2806
Reid I. N., Gizis J. E., 1997, AJ, 113, 2246
Reipurth B., Clarke C., 2001, AJ, 122, 432
Salim S., Gould A., 2003, ApJ, 582, 1011
Ségransan D., Delfosse X., Forveille T., Beuzit J.-L., Udry S., Perrier C., Mayor M., 2000, A&A, 364, 665
Siegler N., Close L. M., Cruz K. L., Martín E. L., Reid I. N., 2005, ApJ, 621, 1023
Simon T., 1990, ApJ, 359, L51
Soderblom D. R., Stauffer J. R., Hudon J. D., Jones B. F., 1993, ApJS, 85, 315
Terndrup D. M., Pinsonneault M., Jeffries R. D., Ford A., Stauffer J. R., Sills A., 2002, ApJ, 576, 950
Tinney C. G., Mould J. R., Reid I. N., 1993, AJ, 105, 1045
Tubbs R. N., Baldwin J. E., Mackay C. D., Cox G. C., 2002, A&A, 387, L21
Umbreit S., Burkert A., Henning T., Mikkola S., Spurzem R., 2005, ApJ, 623, 940
van Altena W. F., Lee J. T., Hoffleit E. D., 2001, VizieR Online Data Catalog, 1238, 0
Voges W. E. A., 1999, VizieR Online Data Catalog, 9010, 0
Voges W. E. A., 2000, VizieR Online Data Catalog, 9029, 0

This paper has been typeset from a TEX/LATEX file prepared by the author.